Available online at www.sciencedirect.com

ScienceDirect

Vision Research 47 (2007) 1682–1692

Vision Research

www.elsevier.com/locate/visres

Binocular influences on global motion processing in the human visual system

R.F. Hess [a,*], C.V. Hutchinson [b], T. Ledgeway [b], B. Mansouri [a]

[a] McGill Vision Research, Department of Ophthalmology, McGill University, 687 Pine Ave W (H4.14), Montreal, PQ, Que., Canada H3A 1A1

[b] Nottingham Visual Neuroscience Group, School of Psychology, University of Nottingham, UK

Received 15 November 2006; received in revised form 23 January 2007

Abstract

This study investigates four key issues concerning the binocular properties of the mechanisms that encode global motion in human vision: (1) the extent of any binocular advantage; (2) the possible site of this binocular summation; (3) whether or not purely monocular inputs exist for global motion perception; (4) the extent of any dichoptic interaction. Global motion coherence thresholds were measured using random-dot-kinematograms as a function of the dot modulation depth (contrast) for translational, radial and circular flow fields. We found a marked binocular advantage of approximately 1.7, comparable for all three types of motion and the performance benefit was due to a contrast rather than a global motion enhancement. In addition, we found no evidence for any purely monocular influences on global motion detection. The results suggest that the site of binocular combination for global motion perception occurs prior to the extra-striate cortex where motion integration occurs. All cells involved are binocular and exhibit dichoptic interactions, suggesting the existence of a neural mechanism that involves more than just simple summation of the two monocular inputs.

Keywords: Global motion; Optic flow; Contrast; Binocular summation; Dichoptic interaction

1. Introduction

Over the past decades, our understanding of the properties of global motion processing (i.e., the integrated direction or speed of a number of elementary, local motions) and its neural substrate (Morgan & Ward, 1980; Siegel & Andersen, 1988; Williams & Sekuler, 1984) has increased considerably. For example, it has been established that the processes that serve to integrate local motions into global percepts of translation and optic flow, can utilize both first-order and second-order image cues (Baker & Hess, 1998; Ledgeway & Hess, 2000) and operate in both central and peripheral vision (Dumoulin, Baker, & Hess, 2001). Furthermore there is much evidence to suggest that the mechanisms mediating global motion perception sum inputs across a wide spatial frequency range (Bex & Dakin, 2002) and have extensive areal (Burr, Morrone, & Vania, 1998; Downing & Movshon, 1989) and temporal (Burr & Santoro, 2001; Downing & Movshon, 1989) summation.

It is presently assumed that the cortical mechanisms underlying global motion analysis are extra-striate because of the large areas over which local motion summation takes place (Burr et al., 1998; Downing & Movshon, 1989). For example, cells in area MT are well-suited to this task as they have large receptive fields, with multiple spatially localized local motion inputs, that are thought to provide the basis of such summation (Movshon, Adelson, Gizzi, & Newsome, 1985). Moreover lesions to this area in monkey (Newsome & Pare, 1988) and its homolog in man (Baker & Hess, 1991) disrupt the ability to encode the direction of global motion. There is also a strong correlation between behavioural performance and cellular responses in this area (Britten, Shadlen, Newsome, & Movshon, 1992) in that performance can be modified in a predictable manner by microstimulation of these cells (Salzman, Murasugi, Britten, & Newsome, 1992).

* Corresponding author. Fax: +1 514 843 1691.
E-mail address: Robert.hess@mcgill.ca (R.F. Hess).

0042-6989/$ - see front matter © 2007 Elsevier Ltd. All rights reserved.
doi:10.1016/j.visres.2007.02.005

The current, widely accepted, view of global motion processing is that it involves at least two processing stages: (1) an initial stage of local motion detection that is contrast-sensitive and (2) a subsequent stage of motion integration that is relatively contrast-invariant (Morrone, Burr, & Vaina, 1995). The first stage has been identified with cells in area V1, whereas the second stage has been identified tentatively with cellular responses in area MT (Movshon et al., 1985; Rodman & Albright, 1989). The available neurophysiological evidence suggests that motion detectors in V1, that respond to local motion in a manner consistent with contrast-energy analysis (Movshon & Newsome, 1996), send their outputs to area MT where there is evidence for cells with broader spatial and orientational responses (Movshon et al., 1985).

It is clear from a number of different standpoints that binocularity plays an important role in global motion processing. For example, the motion after-effect to global motion exhibits, on average, 96% interocular transfer, suggesting a higher level of binocularity than typically found in V1 (Raymond, 1993). Binocular disparity can facilitate global motion direction discrimination (Greenwood & Edwards, 2006; Hibbard & Bradshaw, 1999; Snowden & Rossiter, 1999). Also, developmental conditions in which the binocular function has been compromised due to unilateral amblyopia exhibit anomalous global motion processing for both the affected and fellow fixing eye, suggesting an abnormality at a binocular site (Giaschi, Regan, Kraft, & Hong, 1992; Ho et al., 2005; Simmers, Ledgeway, Hess, & McGraw, 2003). However the extent of the binocular advantage for the perception of global motion and the level at which it arises, is presently indeterminate.

As local motion detection is assumed to be monocular (Georgeson & Shackleton, 1989; Lu & Sperling, 2001), one possibility is that binocular summation for global motion arises beyond V1, perhaps within extra-striate area MT itself where the majority of cells are binocular (Maunsell & Van Essen, 1983; Zeki, 1978). Alternatively as a sizeable population of directionally selective cells in V1 are binocular (Hubel & Weisel, 1968), and there is debate concerning a binocular input to motion perception, it is possible that the V1 cells that project to MT are themselves binocular. Consequently the binocularity of global motion processing in MT could be largely inherited from its first stage (V1) inputs.

In the context of spatial vision, the extent of the binocular advantage for simple form detection is known to be modest, being of the order of 1.4 (Campbell & Green, 1965). On the other hand, for large field low spatial frequency stimuli in motion it can be as large as a factor of 2 (Rose, 1980). The locus of this binocular advantage in sensitivity is unresolved but could arise in either striate or extra-striate cortex, or even a combination of the two. Therefore, in the present study we sought to assess the extent and the site of the binocular advantage for global motion perception in human vision.

To address these issues we measured the relationship between the global motion coherence threshold and stimulus modulation depth (contrast) for stochastic stimuli undergoing translational, radial and circular motion under a range of viewing conditions.

2. Experiment 1. Global motion thresholds under monocular and binocular viewing

In Experiment 1 global motion coherence thresholds versus contrast functions were measured under monocular and binocular viewing conditions using a similar technique to Simmers et al. (2003). If there is a binocular viewing advantage such that thresholds can be measured over a lower contrast range than for monocular viewing (characterized by a lateral shift of the threshold versus contrast function along the contrast axis), this would suggest the locus of this phenomenon is a contrast-dependent site, namely V1. If on the other hand binocular viewing results in a uniform improvement in global motion performance, compared with monocular viewing, at all contrasts tested (characterized by a vertical shift of the threshold versus contrast function along the threshold axis) this would implicate a contrast-invariant site in extra-striate cortex (cf. MT or MSTd).

2.1. Methods

2.1.1. Observers

Three observers took part in Experiment 1. CVH was one of the authors and JT and JB were volunteers naïve to the purpose of the experiment. All had normal or corrected-to-normal visual acuity and normal binocular vision.

2.1.2. Apparatus and stimuli

Stimuli were generated using a *Macintosh G4* and presented on a *Sony Multiscan G520* monitor with an update rate of 75 Hz which was gamma-corrected with the aid of internal look-up tables. The mean luminance of the display was approximately 50 cd/m^2. Stimuli were presented within a circular window at the centre of the display which subtended 12° at the viewing distance of 92 cm.

Global motion stimuli were either translational, radial or rotational random-dot kinematograms (RDKs). Dots were presented on a homogenous mid-grey background (mean luminance of 50 cd/m^2) that filled the entire circular display window. The luminance modulation (Michelson contrast) and hence the visibility of the dots could be varied by increasing the luminance of the dots, with respect to the background, according to the following equation:

$$\text{Dot luminance modulation} = (L_{\text{dots}} - L_{\text{background}})/(L_{\text{dots}} + L_{\text{background}}), \quad (1)$$

where L_{dots} and $L_{background}$ are the dot and background luminances, respectively. The luminance modulation of the dots ranged between 0.004 and 0.33.

Each RDK was generated anew immediately prior to its presentation and was composed of a sequence of eight images, which when presented consecutively produced continuous apparent motion. The duration of each image was 53.3 ms, resulting in a total stimulus duration of 426.7 ms. Each image contained 100 non-overlapping dots (dot density 0.88 dots/deg^2) and the diameter of each dot was 0.235°. At the beginning of each motion sequence, the position of each dot was randomly assigned. On subsequent frames, each dot was shifted by 0.3°, resulting in a drift speed, if sustained, of 5.9°/s. When a dot dropped off the edge of the circular display window it was immediately re-plotted in a random spatial position within the confines of the window.

The global motion coherence level of the stimulus was manipulated by constraining a fixed proportion of 'signal' dots on each image update to move coherently along a trajectory (either translational, radial or rotational) and the remainder ('noise' dots) to move in random directions. In the case of translational motion, signal dot direction could be either upwards or downwards on each trial with equal probability. For radial motion, on each trial signal dots were displaced along trajectories consistent with either expansion or contraction with equal probability. For rotational motion, signal dots rotated either clockwise or anti-clockwise, again with equal probability. Following previous studies that have employed comparable radial and rotational RDK stimuli (Burr & Santoro, 2001), the magnitude of the dot displacement was always constant across space in that it did not vary with distance from the origin as it would for strictly rigid global radial or rotational motion. This ensured that all stimuli were identical in terms of the speeds of the local dots. As such, performance for radial and rotational motion could be directly compared to performance for translational motion.

2.1.3. Procedure

All measurements were carried out under either monocular or binocular viewing conditions. In the monocular viewing condition, measurements were repeated with both the left eye and the right eye. In this instance, the other eye was occluded using an eye patch. In the binocular viewing condition, observers viewed the same stimulus but with both eyes. Global motion thresholds were measured using a single-interval, forced-choice, direction-discrimination procedure. On each trial, observers were presented with an RDK stimulus in which the signals dots moved along either a translational, radial or rotational trajectory. Performance was measured separately for each of the motion types and the order of testing was randomized. For translational motion, the observers' task was to identify whether the motion was upwards or downwards. For radial motion, the task was to identify whether the motion was expansion or contraction and for rotational motion, the task was to identify whether the dots rotated clockwise or anti-clockwise. Data-collection was carried out using an adaptive staircase procedure (Edwards & Badcock, 1995). The staircase varied the proportion of signal dots present on each trial, according to the observer's recent response history. The staircase terminated after eight reversals and thresholds (79% correct performance) were taken as the mean of the last six reversals. Each threshold reported is based on the mean of at least five staircases. For the monocular viewing condition, the results for the left and right eyes were combined and a mean was taken.

2.2. Results

Figs. 1–3 plot global motion coherence thresholds (expressed as the % signal dots) for discriminating the direction of translational, radial and rotational motion, respectively. Thresholds are plotted as a function of the dot modulation depth (contrast) under monocular (average of left and right eyes) and binocular viewing conditions.

The general form of the relationship between the coherence threshold and the dot modulation depth is similar in all cases and is well described by a power function plus a constant (Simmers et al., 2003):

$$y = ax^b + c, \tag{2}$$

where a, b, and c are constants (Simmers et al., 2003) and the derived parameters are displayed in Table 1.

Thresholds are lower for binocular than for monocular viewing at the lowest contrasts tested and it is apparent from inspection of the data that the function describing the average monocular results is to a first approximation simply shifted horizontally along the contrast axis. To quantify this relationship we utilized a two-parameter model based on Eq. (2). The parameters determine the relative lateral (i.e., contrast-dependent) and vertical (i.e., signal-to-noise-dependent) shifts needed to superimpose the monocular and binocular data sets (see Simmers et al., 2003 for details). This analysis determines the ratio of the best fitting parameters describing the lateral (contrast or visibility) and vertical (global motion sensitivity) shifts needed to bring the monocular and binocular functions into correspondence.

Fig. 4 plots the average derived monocular/binocular performance ratios for the contrast (horizontal shift) and motion (vertical shift) components using the procedure outlined above. Each plot is for a different motion type: translational, radial and rotational. It is apparent that a marked contrast component shift of about a factor of 1.7 is required to align the binocular and monocular data for each of the three types of motion. However, the magnitude of the motion component shift is close to unity (in relation to the magnitude of the error bars) confirming that the binocular and monocular curves are principally related to each other by a contrast

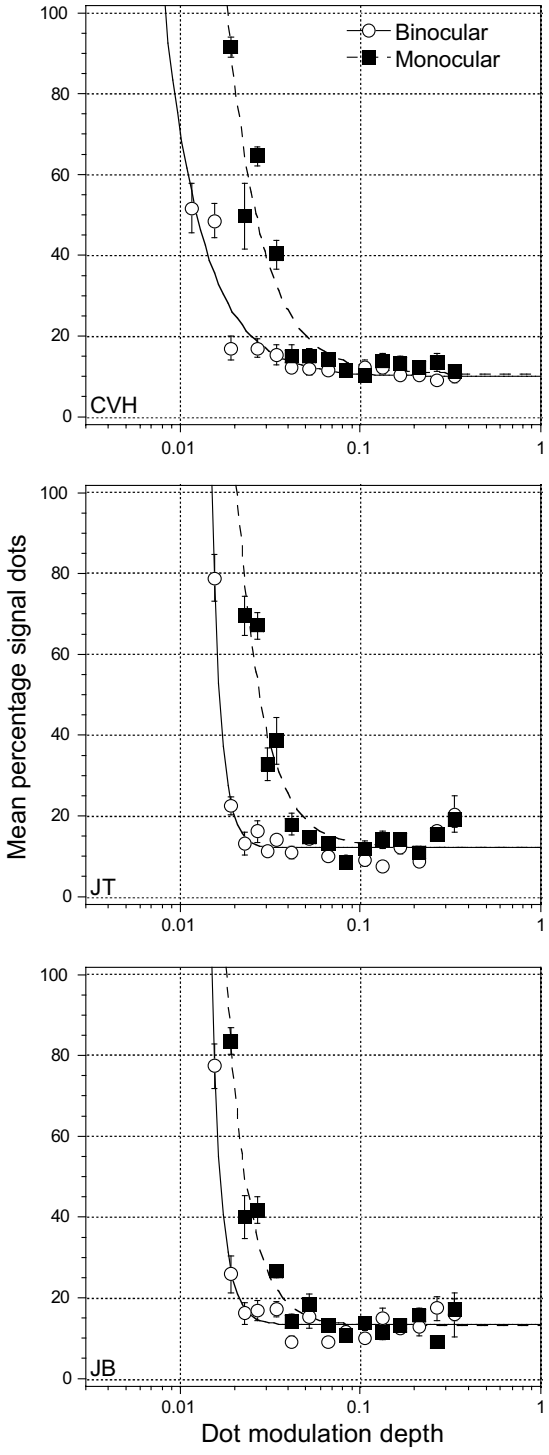

Fig. 1. Global motion thresholds (mean percentage of signal dots required to elicit 79% correct performance) for three observers (CVH, JT & JB) for identifying the direction of translational motion. These are plotted as a function of dot modulation depth under conditions of either monocular (squares) or binocular (circles) viewing. The data have been fitted with a power function plus a constant. Error bars represent ±1 SEM.

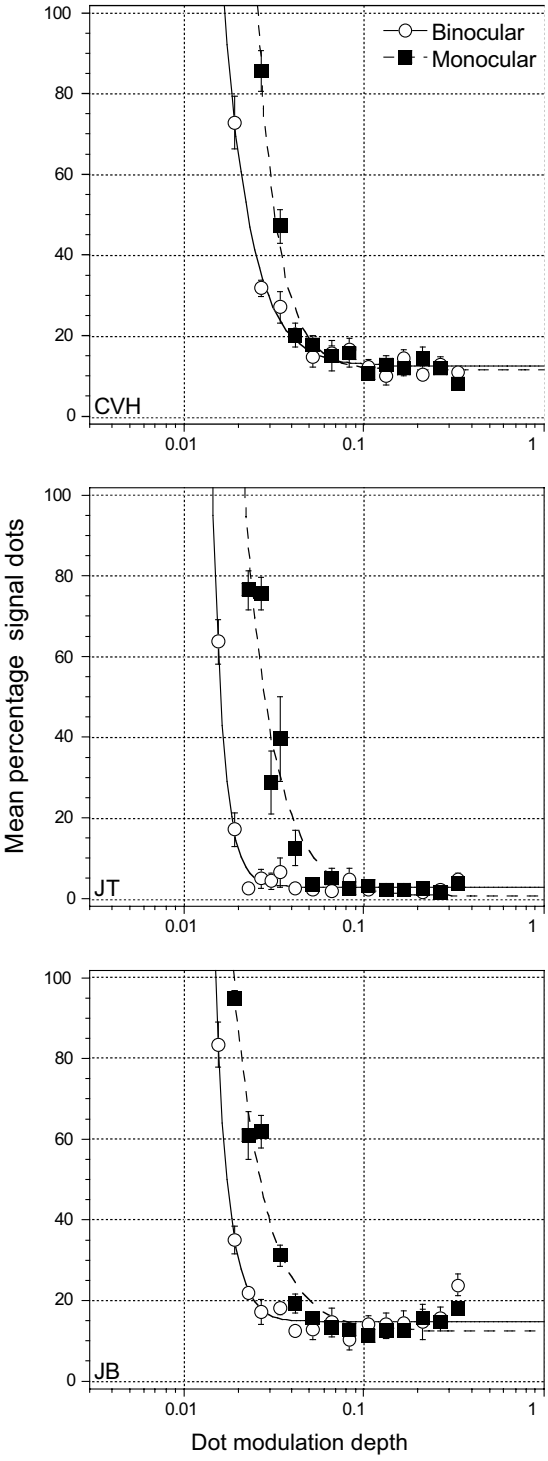

Fig. 2. Global motion thresholds (mean percentage of signal dots required to elicit 79% correct performance) for three observers (CVH, JT & JB) for identifying the direction of radial motion. These are plotted as a function of dot modulation depth under conditions of either monocular (squares) or binocular (circles) viewing. The data have been fitted with a power function plus a constant. Error bars represent ±1 SEM.

scaling factor. This implies that for global motion perception the advantage of binocular viewing over monocular viewing is determined by a process that is sensitive to image contrast.

3. Experiment 2. Global motion thresholds under dichoptic viewing

Our results so far address the site and extent of the binocular advantage for global motion processing which could

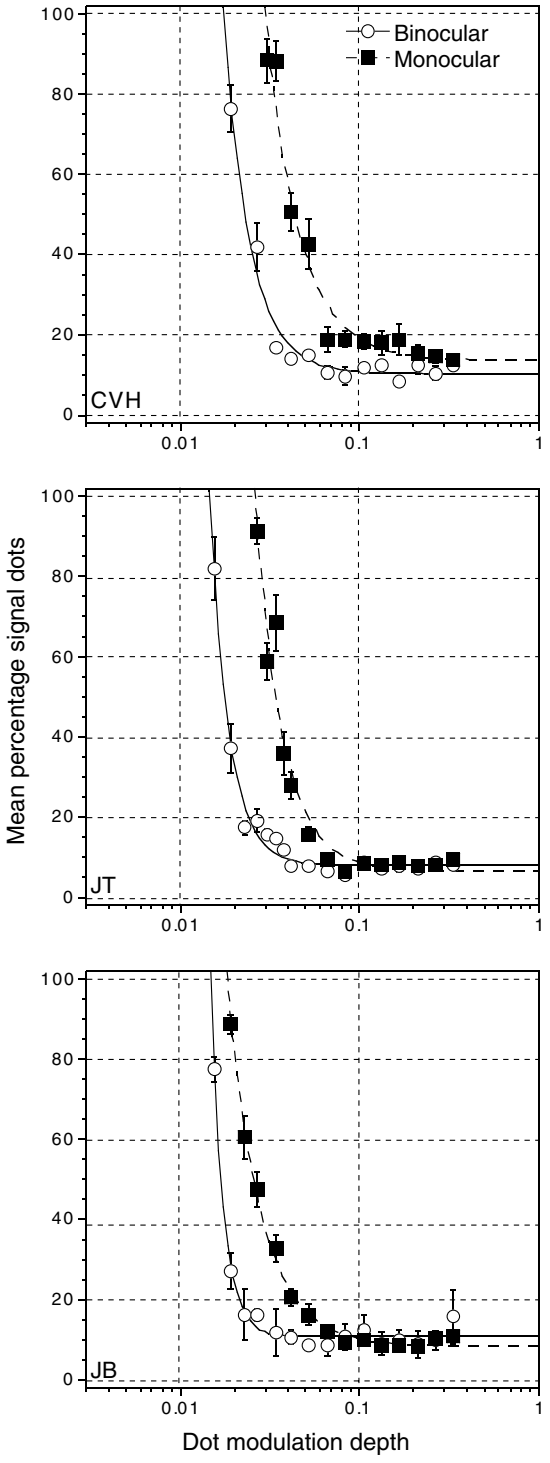

Fig. 3. Global motion thresholds (mean percentage of signal dots required to elicit 79% correct performance) for three observers (CVH, JT & JB) for identifying the direction of rotational motion. These are plotted as a function of dot modulation depth under conditions of either monocular (squares) or binocular (circles) viewing. The data have been fitted with a power function plus a constant. Error bars represent ±1 SEM.

be mediated solely by binocular cells. However the possibility remains that the monocular performance could be determined in whole, or in part, by monocularly activated cells of equal or reduced sensitivity compared with their binocular counterparts. That is, we sought to investigate (1) if there are any purely monocular inputs for global motion perception and (2) if a simple summing circuit involving the monocular inputs would suffice to explain binocular influences on global motion perception.

To address these issues we investigated global motion detection using a dichoptic stimulation paradigm, in which the signal dots were presented to one eye and the noise dots were simultaneously presented to the other eye. If purely monocular global motion-detecting mechanisms exist, then coherence thresholds driven by mechanisms in one eye should be independent of the noise seen by mechanisms activated by the other eye and as a result much lower thresholds (i.e., approximating one signal element) should be found in the dichoptic case.

3.1. Methods

3.1.1. Observers

Three observers (CVH, BM & AR) took part in the main experiments; CVH and BM were authors and AR was a naïve participant. Five other observers (MM, CAS, PCH, EG, BST) took part in the comparison of monocular and dichoptic thresholds (Fig. 9). All had normal or corrected-to-normal visual acuity and normal binocular vision.

3.1.2. Apparatus and stimuli

As in Experiment 1, global motion stimuli were either translational, radial or rotational RDKs. Stimuli were generated using a *Macintosh G4* and presented on a *Sony Professional Series P22f* monitor with an update rate of 75 Hz which was gamma-corrected with the aid of internal look-up tables. The mean luminance of the display was $\sim$55 cd/m^2. The RDKs were presented within two horizontally separated, circular display windows, each equidistant from the centre of the screen. Images were viewed at a distance of 114 cm through a Wheatstone Stereoscope. Each circular window subtended 7° and to aid binocular fusion, each display region was surrounded by a rectangular frame.

Dots were presented on a homogenous mid-grey background. The luminance modulation (Michelson contrast) and hence the visibility of the dots could be varied by increasing the luminance of the dots, with respect to the background in an identical manner to Experiment 1.

Although the image sizes were different in the two experiments, to keep Experiments 1 and 2 as comparable as possible, in Experiment 2, stimulus parameters were such that dot radius, dot density, dot speed and dot displacement remained the same as in Experiment 1. Therefore, in Experiment 2, each circular display window contained 35 non-overlapping dots.

Threshold performance was measured for each type of global motion (translational, radial and rotational) under three viewing conditions (monocular, dichoptic and binocular). Each viewing condition contained two images (see

Table 1
Model parameters for three observers (CVH, JT & JB) for the three types of motion (translation, radial and rotation) under the two viewing conditions (monocular and binocular) in Experiment 1

Observer	Motion type	Viewing condition	Constants		
			a	*b*	*c*
CVH	Translation	Monocular	1.1868^{e-02} (2.1638^{e-02} SEM)	−2.2306 (0.46579 SEM)	10.535 (3.2843 SEM)
		Binocular	1.3928^{e-02} (1.302^{e-02} SEM)	−1.8094 (0.19419 SEM)	9.5365 (1.7273 SEM)
	Radial	Monocular	6.5273^{e-03} (9.2822^{e-03} SEM)	−2.5346 (0.3794 SEM)	9.988 (2.6273 SEM)
		Binocular	6.9766^{e-03} (5.1905^{-03} SEM)	−2.2725 (0.17956 SEM)	11.289 (1.2707 SEM)
	Rotation	Monocular	2.8546^{e-02} (3.9229^{-02} SEM)	−2.2817 (0.39299 SEM)	13.59 (3.0459 SEM)
		Binocular	9.0978^{-03} (9.6463^{-03} SEM)	−2.2207 (0.25591 SEM)	9.0976 (1.977 SEM)
JT	Translation	Monocular	1.1812^{e-03} (2.6624^{-03} SEM)	−2.8895 (0.60366 SEM)	12.173 (2.55 SEM)
		Binocular	6.4205^{e-14} (4.0015^{e-13} SEM)	−8.2989 (1.4835 SEM)	11.98 (1.0158 SEM)
	Radial	Monocular	4.4307^{e-03} (8.7154^{e-03} SEM)	−2.6126 (0.52707 SEM)	2.7726 (0.51925 SEM)
		Binocular	7.8968^{e-12} (2.0288^{e-11} SEM)	−7.1219 (0.61261 SEM)	2.7726 (0.51925 SEM)
	Rotation	Monocular	3.0646^{-03} (4.7965^{-03} SEM)	−2.8305 (0.43692 SEM)	6.5022 (2.7462 SEM)
		Binocular	2.3923^{e-06} (2.8326^{-06} SEM)	−4.1375 (0.28442 SEM)	8.051 (0.7358 SEM)
JB	Translation	Monocular	7.0069^{e-05} (1.0474^{e-04} SEM)	−3.4922 (0.51157 SEM)	13.095 (1.6164 SEM)
		Binocular	5.0534^{e-12} (2.0208^{e-11} SEM)	−7.241 (0.95337 SEM)	13.268 (0.84814 SEM)
	Radial	Monocular	4.0631^{e-03} (5.2272^{e-03} SEM)	−2.5167 (0.32867 SEM)	12.363 (2.047 SEM)
		Binocular	5.8453^{e-10} (1.2657^{-09} SEM)	−6.1103 (0.51729 SEM)	10.722 (0.65246 SEM)
	Rotation	Monocular	9.5471^{-03} (3.532^{-03} SEM)	−2.2897 (0.094521 SEM)	8.3461 (0.6506 SEM)
		Binocular	1.1676^{-07} (6.1574^{-07} SEM)	−4.7362 (1.2589 SEM)	1.1846 (2.3355 SEM)

The relationship between the global motion threshold and dot modulation depth is well described by a power function plus a constant as follows: $y = ax^b + c$, where a, b and c are constants.

Fig. 5). In the monocular viewing condition, the signal and noise dots were presented to one eye and a uniform grey field of mean luminance was presented to the other eye. In the dichoptic viewing condition, the signal dots were presented to one eye and the noise dots were presented to the other eye. In the binocular viewing condition, the two images were identical (i.e., both the signal and the noise dots were correlated in both eyes).

3.1.3. Procedure

Measurements were carried out under monocular, dichoptic and binocular viewing conditions using an analogous procedure to that employed in Experiment 1 with the following exceptions. In the monocular and dichoptic viewing conditions, measurements were repeated with either the left eye or the right eye within the same run of trials. In the dichoptic condition, the signal dots were presented to the left eye in one of the interleaved staircases and to the right eye in the other staircase. In this instance, performance was tracked and thresholds (79% correct performance) determined for each eye using two interleaved adaptive staircase procedures. Each threshold reported is based on the mean of at least six staircases. For the monocular and dichoptic viewing conditions, the results for the left and right eyes were combined.

3.2. Results

Figs. 6–8 plot global motion coherence thresholds (expressed as the % signal dots) for discriminating the direction of translational, radial and rotational motion, respectively. Thresholds are plotted as a function of dot modulation depth (contrast) under monocular, dichoptic and binocular viewing conditions.

The curves represent fits using Eq. (2) described above and the derived parameters of the fits are listed in Table 2. It is evident that similar performance is obtained in the monocular and dichoptic conditions. There is no indication that performance is substantially better in the dichoptic than the monocular conditions (even at the lowest dot contrast levels at which thresholds could be measured), as one would expect if there were purely monocular mechanisms, however insensitive, capable of detecting the direction of these global motion stimuli. These results provide compelling evidence that there are only binocular mechanisms underlying global motion detection, a conclusion similar to our previous study on global form integration (Mansouri, Hess, Allen, & Dakin, 2005).

The above comparison was between averaged monocular and averaged dichoptic performance, Fig. 9 shows results comparing left and right monocular performance with dichoptic results where the signal was in the left or the right eye. Results are displayed for eight subjects in which coherence threshold (filled and unfilled bars, dot modulation depth is given in caption) is plotted against the eye that viewed the dichoptic *signal* (the other eye viewing the noise). In all cases, the effectiveness of the signal depended on which eye viewed the signal. To ascertain whether this was monocular or dichoptic in origin, compare these results with the monocular thresholds (vertical and horizontal hatched bars) where signal and noise were in the same eye. A different relationship is found for purely monocular stimulation. The monocular

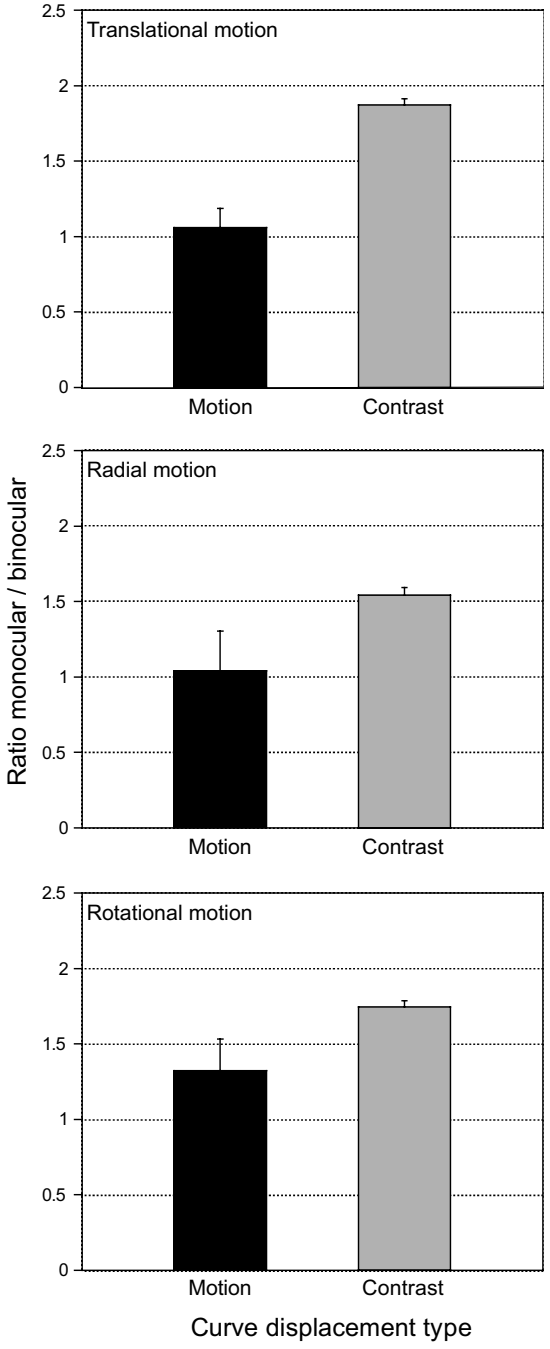

Fig. 4. Comparison of the relative horizontal (contrast-axis) and vertical (motion-axis) displacements required to bring the binocular data (relating motion coherence and dot modulation) into alignment with its monocular counterpart. Averaged results ($n = 3$) with their associated standard errors are compared for the three types of global motion; translation, radial and rotation.

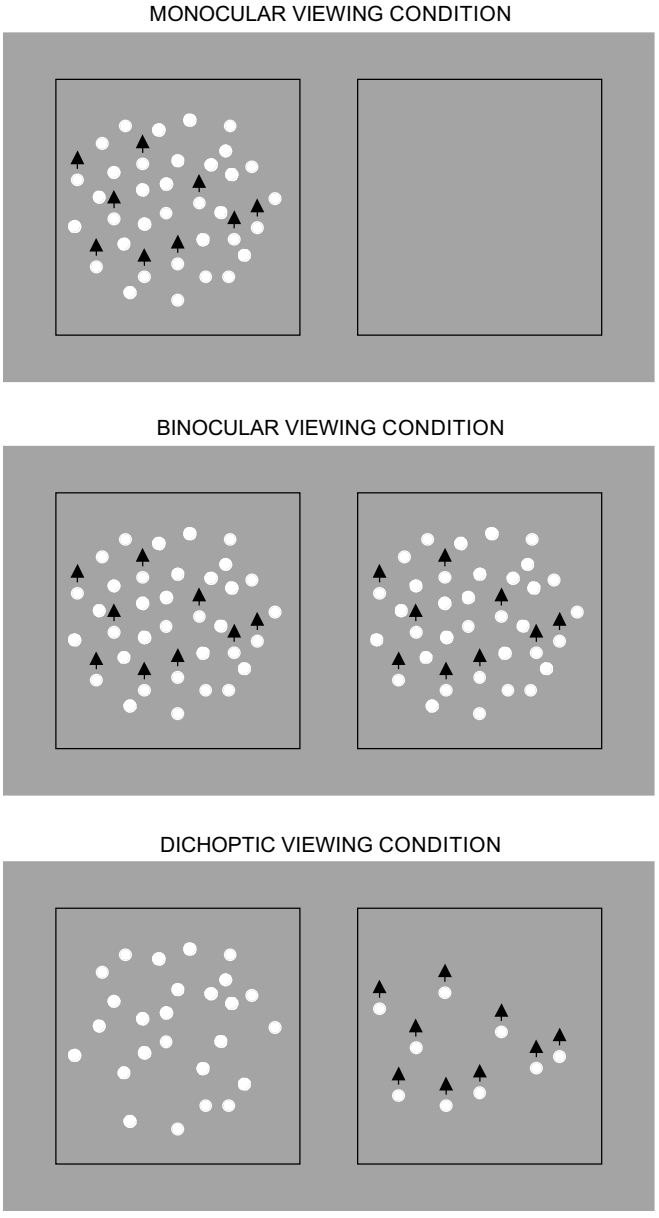

Fig. 5. Schematic of stimulus configuration in Experiment 2. In the monocular viewing condition, the signal and noise were presented to one eye (could be either the left or the right eye with equal probability) and a uniform grey field was presented to the other eye. In the dichoptic viewing condition, the signal was presented to one eye (could be either eye with equal probability) and the noise was presented to the other eye. In the binocular viewing condition, both the signal and the noise were simultaneously presented to both eyes. For demonstration purposes, translational motion is shown as is the motion direction (arrows) of the signal elements. The other elements without arrows are meant to signify the random directions of the noise elements. However, performance for discriminating the direction of radial and rotational global motion was also measured.

performance for each eye is approximately equal and corresponds to the mean of the dichoptic result. This suggests that the left/right eye performance imbalance we found in the dichoptic task does not have a purely monocular basis and therefore must reflect an interaction at a dichoptic/binocular site and not a simple summation of excitatory monocular inputs.

4. Discussion

The results of the present experiments are important in that they clearly elucidate the role of monocular and binocular influences on global motion perception. Specifically, the results lead to four main conclusions: (1) the binocular

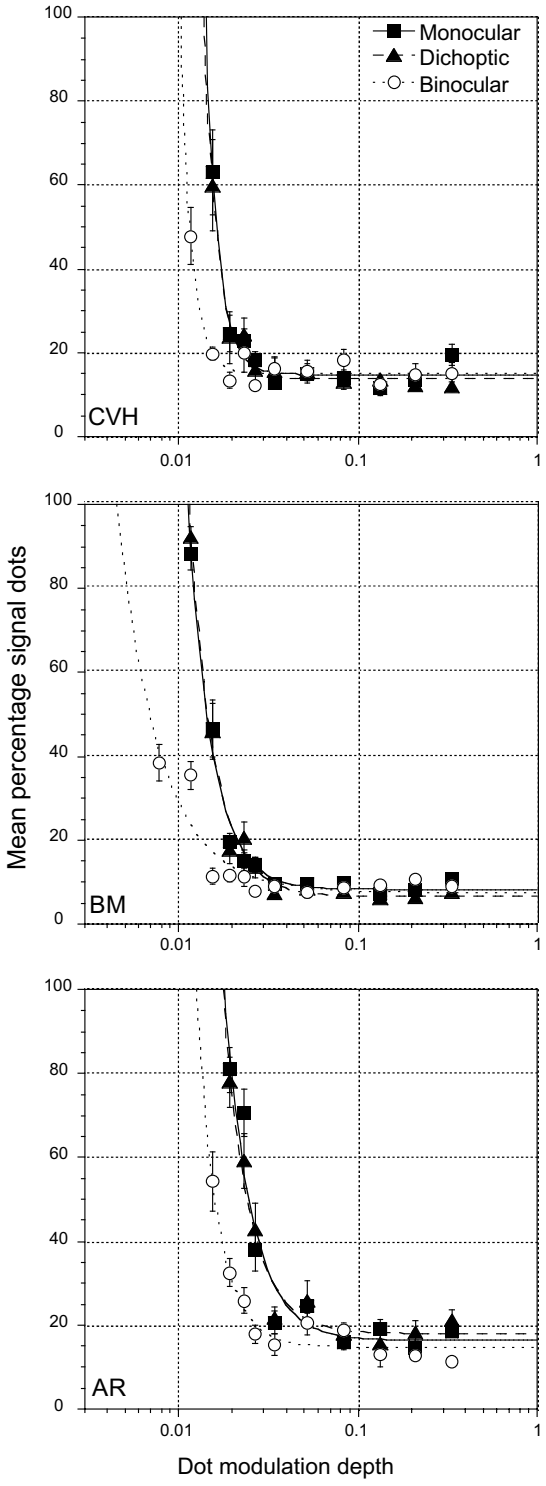

Fig. 6. Global motion thresholds (mean percentage of signal dots required to elicit 79% correct performance) for three observers (CVH, BM & AR) for identifying the direction of translational motion as a function of dot modulation depth under monocular (circles), dichoptic (squares) and binocular (triangles) viewing conditions. The data have been fitted with a power function plus a constant. Error bars represent ±1 SEM.

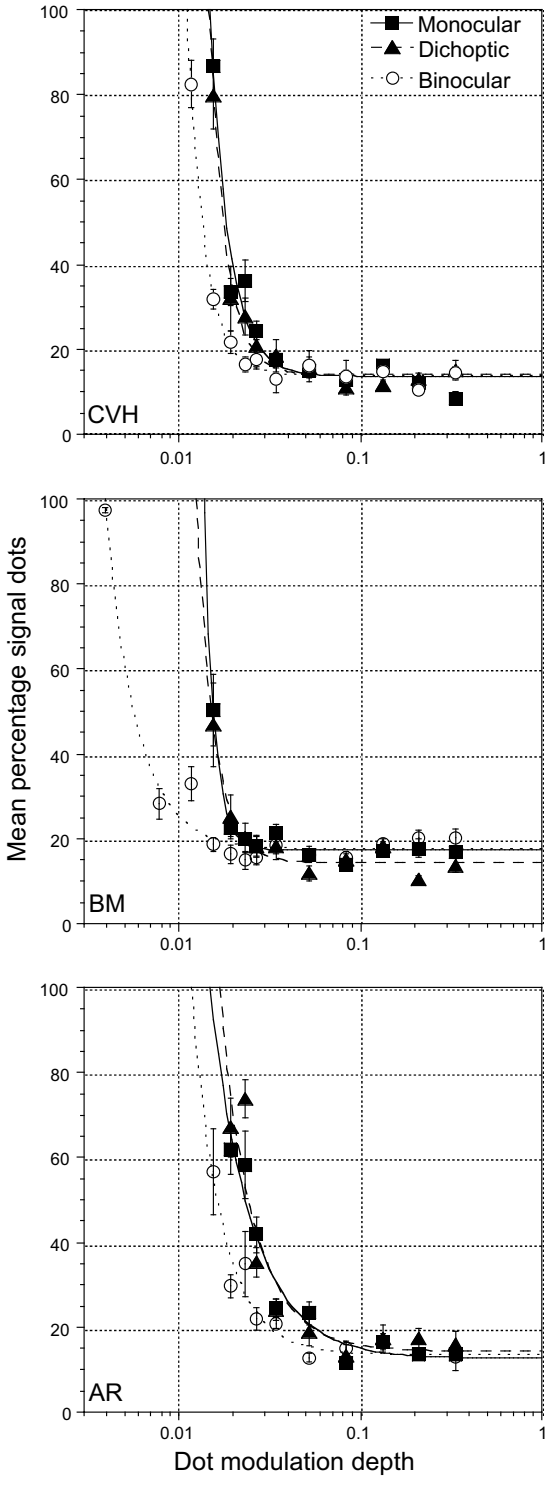

Fig. 7. Global motion thresholds (mean percentage of signal dots required to elicit 79% correct performance) for three observers (CVH, BM & AR) for identifying the direction of radial motion as a function of dot modulation depth under monocular (circles), dichoptic (squares) and binocular (triangles) viewing conditions. The data have been fitted with a power function plus a constant. Error bars represent ±1 SEM.

advantage for global motion coherence is about a factor of 1.7; (2) the probable site of this binocular advantage is striate rather than extra-striate cortex because it is contrast-dependent and does not reflect a uniform motion advantage *per se*; (3) binocularly activated neurons appear to dominate global motion detection in human vision because

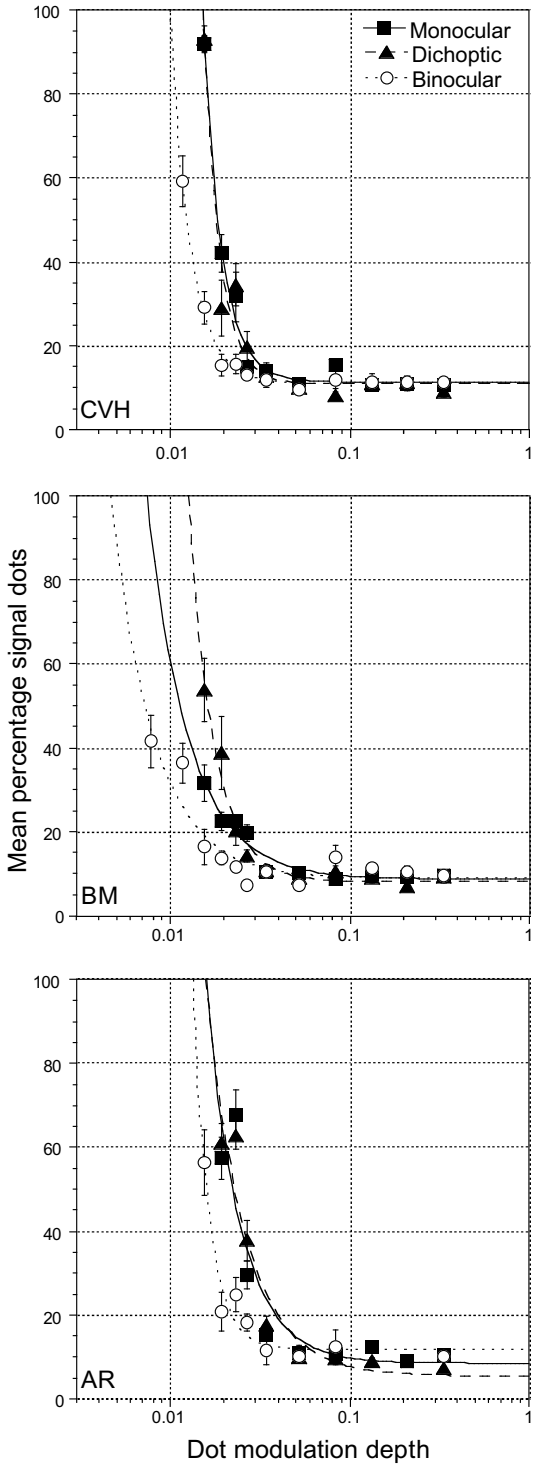

Fig. 8. Global motion thresholds (mean percentage of signal dots required to elicit 79% correct performance) for three observers (CVH, BM & AR) for identifying the direction of rotational motion as a function of dot modulation depth under monocular (circles), dichoptic (squares) and binocular (triangles) viewing conditions. The data have been fitted with a power function plus a constant. Error bars represent ±1 SEM.

dichoptic thresholds, on average, are not substantially lower than monocular thresholds; (4) the binocular circuitry involves more than a simple summation of the two monocular inputs, as dichoptic interactions occur.

There is a long history of assessing the advantage of using two eyes rather than one. Early studies (Campbell & Green, 1965) were based on a theoretical signal-to-noise analysis in which having signal and uncorrelated noise in two eyes led to 2× signal and $\sqrt{2}$× the sum of the monocular variances, hence a $\sqrt{2}$ or 1.4 binocular advantage in signal-to-noise. Later models (Legge, 1984a) incorporated a response non-linearity prior to summation. If the monocular response non-linearity to contrast is expressed by an exponent q, the predicted improvement in binocular contrast detection is therefore $2^{(1/q)}$. When $q = 2$ this represents the monocular contrast energy and, results in quadratic binocular summation (i.e., 1.4). Although both analyses predict a binocular advantage of $\sqrt{2}$, recent investigations of the spatiotemporal parameter space suggests it is actually closer to 1.7 (Georgeson, Meese, & Baker, 2005). Larger degrees of binocular summation have been shown for the direction discrimination of large fields of translational motion (Rose, 1980). Depending on the temporal conditions this can be a factor of 2 (Rose, 1980) or even higher (Hess, unpublished). The present estimate of a binocular advantage of 1.7 is comparable to that previously found for contrast thresholds but smaller than the previously reported estimate for direction discrimination where the field size is larger and lower spatial frequencies are involved (Rose, 1980).

An important result of the present study was that the binocular advantage for global motion processing was mainly a contrast, rather than a motion-integration, dependent phenomenon, suggesting a site at the first stage of local motion extraction (i.e., V1). While it is true that binocularity increases as one goes from V1 to MT, this finding suggests that the subset of cells in V1 projecting to MT must be exclusively binocular. If this is indeed the case then previous conclusions on the probable site of interocular transfer following adaptation to global motion (Raymond, 1993) may need to be rethought. The site of such complete transfer may reflect the binocular properties of a specialized subset of cells in V1 that project to MT rather than MT cells *per se*.

In normal vision global motion coherence thresholds are likely to be determined by binocular mechanisms, as in the present study we found no evidence for even an attenuated monocular contribution (as shown by comparable performance under monocular and dichoptic viewing conditions). This finding is perhaps not surprising given that extra-striate visual areas such as MT and MSTd contain cells that are mostly or exclusively binocular (Maunsell & Van Essen, 1983; Zeki, 1978). This notion is entirely consistent with the proposition that only binocular V1 cells project to MT, where the integration of local motions by global pooling mechanisms first take place. It would appear that only when binocular vision is compromised in early visual development, for example due to a strabismus, that monocular cells are found in these extra-striate areas (Schroder, Fries, Roelfsema, Singer, & Engel, 1998, 2002). In these cases, global motion coherence thresholds are anomalous for

Table 2
Model parameters for three observers (CVH, BM & AY) for the three types of motion (translation, radial and rotation) under the three viewing conditions (monocular, dichoptic and binocular) in Experiment 2

Observer	Motion type	Viewing condition	Constants		
			a	*b*	*c*
CVH	Translation	Monocular	3.971^{e-10} (1.7755^{e-09} SEM)	−6.1234 (1.0668 SEM)	14.84 (1.2193 SEM)
		Dichoptic	6.2987^{e-09} (3.3034^{e-08} SEM)	−5.4485 (0.86383 SEM)	13.774 (1.1517 SEM)
		Binocular	3.7976^{e-12} (3.3034^{e-11} SEM)	−6.6914 (1.9396 SEM)	15.072 (0.95203 SEM)
	Radial	Monocular	3.8808^{e-06} (1.1317^{e-05} SEM)	−4.0135 (0.6991 SEM)	13.647 (2.3598 SEM)
		Dichoptic	1.4371^{e-07} (3.4218^{-07} SEM)	−4.7818 (0.56962 SEM)	14.16 (1.3344 SEM.)
		Binocular	9.7247^{e-08} (1.3587^{-07} SEM)	−4.5772 (0.31256 SEM)	13.98 (0.68401 SEM)
	Rotation	Monocular	2.1173^{e-06} (3.2158^{-06} SEM)	−4.1891 (11.376 SEM)	11.376 (1.306 SEM)
		Dichoptic	2.3605^{e-07} (8.4893^{-07} SEM)	−4.7151 (0.86049 SEM)	10.892 (2.5643 SEM)
		Binocular	2.1947^{-06} (2.5968^{-06} SEM)	−3.7994 (0.26518 SEM)	1.101 (0.57122 SEM)
BM	Translation	Monocular	5.2355^{e-05} (6.2682^{-05} SEM)	−3.2027 (0.2688 SEM)	8.2147 (1.2899 SEM)
		Dichoptic	7.7511^{e-065} (9.1273^{-05} SEM)	−3.1276 (0.26445 SEM)	6.6811 (1.3974 SEM)
		Binocular	4.566^{e-03} (1.2419^{e-02} SEM)	−1.8366 (7.6035 SEM)	7.6035 (2.3275 SEM)
	Radial	Monocular	6.4559^{e-13} (4.2569^{-12} SEM)	−7.5743 (1.5699 SEM)	17.285 (0.82698 SEM)
		Dichoptic	3.9856^{-07} (1.3963^{e-06} SEM)	−4.3687 (0.83902 SEM)	14.368 (1.1234 SEM)
		Binocular	8.7616^{-05} (0.000195 SEM)	−2.4763 (0.40008 SEM)	17.535 (1.4817 SEM)
	Rotation	Monocular	1.0737^{-02} (1.7646^{-02} SEM)	−1.8416 (0.39593 SEM)	8.6752 (1.2501 SEM)
		Dichoptic	1.6916^{-04} (2.9492^{-04} SEM)	−3.0112 (0.41944 SEM)	8.0126 (1.4258 SEM)
		Binocular	5.2712^{e-03} (1.2979^{e-02} SEM)	−1.8173 (0.50788 SEM)	8.877 (2.2535 SEM)
AR	Translation	Monocular	7.4642^{e-04} (2.1514^{e-03} SEM)	−2.8959 (0.73311 SEM)	16.405 (3.7215 SEM)
		Dichoptic	5.772^{e-04} (1.1444^{e-03} SEM)	−2.9342 (0.50425 SEM)	17.976 (2.2651 SEM)
		Binocular	1.046^{e-05} (2.9091^{e-05} SEM)	−3.6347 (0.66757 SEM)	14.745 (1.4492 SEM)
	Radial	Monocular	3.202^{e-02} (5.5981^{e-02} SEM)	−1.8779 (0.44349 SEM)	12.628 (3.0482 SEM)
		Dichoptic	6.515^{e-03} (2.3024^{-02} SEM)	−2.3133 (0.89908 SEM)	14.428 (5.304 SEM.)
		Binocular	7.4937^{e-04} (2.2837^{-03} SEM)	−2.6191 (0.72875 SEM)	13.597 (3.1075 SEM)
	Rotation	Monocular	6.4732^{-03} (2.5736^{-02} SEM)	−2.3033 (1.0114 SEM)	8.4978 (5.7303 SEM)
		Dichoptic	2.1901^{e-02} (5.88^{-02} SEM)	−2.0156 (0.67848 SEM)	5.4747 (5.5473 SEM)
		Binocular	1.1676^{-07} (6.1574^{-07} SEM)	−4.7362 (1.2589 SEM)	1.1846 (2.3355 SEM)

Once more, the relationship between the global motion threshold and dot modulation depth is well described by a power function plus a constant as follows: $y = ax^b + c$, where a, b and c are constants.

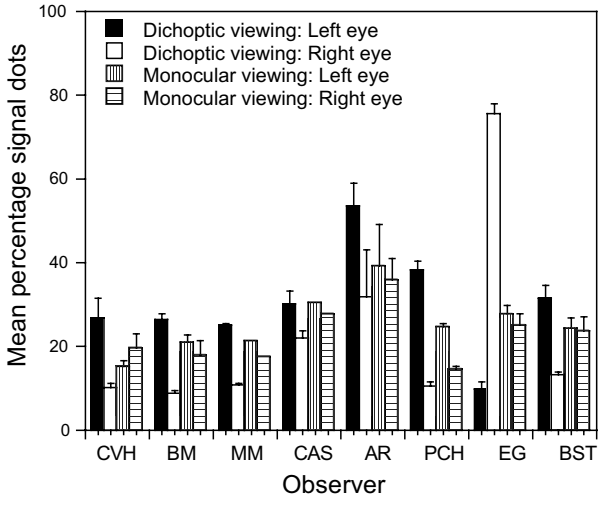

Fig. 9. Global motion thresholds (mean percentage of signal dots required to elicit 79% correct performance) for eight observers for identifying the direction of rotational motion as a function of dot modulation depth (fixed at 0.02 for all subjects except for CVH where it was 0.03) under monocular (hatched bars, just for CVH, BM & AY), dichoptic (filled and unfilled bars) viewing conditions. For the dichoptic conditions, the eye indicated in the legend was presented with signal dots, the other eye received noise dots only. Error bars represent ±1 SEM.

both the fixing and fellow amblyopic eye stimulation (Simmers et al., 2003).

Another interesting finding was the imbalanced performance in the dichoptic task with better performance being obtained when noise was presented to a particular eye. We ruled out the possibility that this dichoptic difference was due to purely monocular sensitivity differences, for example due to more superior retinal processing in one eye. These results suggest therefore that the binocular summation circuit for binocular global motion mechanisms is not just a simple summation of the two excitatory monocular inputs. These results suggest additional dichoptic influences. For example, one possibility is that the reason why the visual system does not have purely monocular access to global motion signals under the conditions of our experiment is that uncorrelated signals (in our case, noise) from the other eye initiates interocular inhibitory interactions at or before the site where motion is binocularly integrated. The reason why these posited inhibitory interactions are not balanced between the eyes is, however, unclear. On a previous occasion, using a global orientation task (Mansouri et al., 2005), we found a similar effect, namely an imbalanced dichoptic effect that corresponded to a more disruptive effect of noise when it came through one or other of the eye.

Acknowledgments

This work was supported by an NSERC (# 46528-06) and CIHR Grants (# MOP 53346) to RFH.

References

Baker, C. L., & Hess, R. F. (1998). Two mechanisms underlie processing of stochastic motion stimuli. *Vision Research, 38*(9), 1211–1222.

Baker, C. L., Hess, R. F., & Zihl, J. (1991). Residual motion perception in a "motion-blind" patient, assessed with limited-lifetime random dot stimuli. *The Journal of Neuroscience, 11*(2), 454–461.

Bex, P. J., & Dakin, S. C. (2002). Comparison of the spatial-frequency selectivity of local and global motion detectors. *Journal of the Optical Society of America. A, Optics, Image Science, and Vision, 19*(4), 670–677.

Britten, K. H., Shadlen, M. N., Newsome, W. T., & Movshon, J. A. (1992). The analysis of visual motion: a comparison of neuronal and psychophysical performance. *The Journal of Neuroscience, 12*, 4745–4765.

Burr, D. C., Morrone, M. C., & Vania, L. M. (1998). Large receptive fields for optic flow detection in humans. *Vision Research, 38*, 1731–1743.

Burr, D. C., & Santoro, L. (2001). Temporal integration of optic flow, measured by contrast and coherence thresholds. *Vision Research, 41*, 1891–1899.

Campbell, F. W., & Green, D. G. (1965). Monocular versus binocular visual acuity. *Nature, 208*(6), 191–192.

Downing, C. J., & Movshon, J. A. (1989). Spatial and temporal summation in the detection of motion i stochastic random dor displays. *Investigative Ophthalmology & Visual Science, 30*(suppl), p72.

Dumoulin, S. O., Baker, C. L. J., & Hess, R. F. (2001). A centrifugal bias for 2nd order but not 1st order motion. *Journal of the Optical Society of America A, 18*(9), 2179–2189.

Edwards, M., & Badcock, D. R. (1995). Global motion perception: No interaction between the first- and second-order pathways. *Vision Research, 35*, 2589–2602.

Georgeson, M. A., Meese, T. S., & Baker, D. H. (2005). Binocular summation, dichoptic masking and contrast gain control. *Journal of Vision, 5*, 797a.

Georgeson, M. A., & Shackleton, T. M. (1989). Monocular motion sensing, binocular motion perception. *Vision Research, 29*(11), 1511–1523.

Giaschi, D. E., Regan, D., Kraft, S. P., & Hong, X. H. (1992). Defective processing of motion-defined form in the fellow eye of patients with unilateral amblyopia. *Investigative Ophthalmology & Visual Science, 33*, 2483–2489.

Greenwood, J. A., & Edwards, M. (2006). Pushing the limits of transparent-motion detection with binocular disparity. *Vision Research, 46*(16), 2615–2624.

Hibbard, P. B., & Bradshaw, M. F. (1999). Does binocular disparity facilitate the detection of transparent motion? *Perception, 28*(2), 183–191.

Ho, C. S., Giaschi, D. E., Boden, C., Dougherty, R., Cline, R., & Lyons, C. (2005). Deficient motion perception in the fellow eye of amblyopic children. *Vision Research, 45*(12), 1615–1627.

Hubel, D. H., & Weisel, T. N. (1968). Receptive fields and functional architecture of monkey striate cortex. *The Journal of Physiology (London), 195*, 215–243.

Ledgeway, T., & Hess, R. F. (2000). The properties of the motion-detecting mechanisms mediating perceived direction in stochastic displays. *Vision Research, 40*(26), 3585–3597.

Legge, G. E. (1984a). Binocular contrast summation-I. Detection and discrimination. *Vision Research, 24*, 373–383.

Lu, Z. L., & Sperling, G. (2001). The three-systems theory of human visual motion perception:review and update. *Journal of the Optical Society of America A, 13*(12), 2305–2370.

Mansouri, B., Hess, R. F., Allen, H. A., & Dakin, S. C. (2005). Integration, segregation, and binocular combination. *Journal of the Optical Society of America. A, Optics, Image Science, and Vision, 22*(1), 38–48.

Maunsell, J. H., & Van Essen, D. C. (1983). Functional properties of neurons in middle temporal visual area of the macaque monkey. II. Binocular interactions and sensitivity to binocular disparity. *Journal of Neurophysiology, 49*(5), 1148–1167.

Morgan, M. J., & Ward, R. (1980). Conditions for motion flow in dynamic visual noise. *Vision Research, 20*, 431–435.

Morrone, M. C., Burr, D. C., & Vaina, L. M. (1995). Two stages of visual motion processing for radial and circular motion. *Nature, 376*, 507–509.

Movshon, J. A., Adelson, E. H., Gizzi, M. S., & Newsome, W. T. (1985). The analysis of moving visual patterns. In: C. Chagas, R. Gattass, & C. Gross (Eds.), *Pattern recognition mechanisms* (pp. 117–151). Rome: Vatican Press.

Movshon, J. A., & Newsome, W. T. (1996). Visual response properties of striate cortical neurons projecting to area MT in Macague Monkeys. *The Journal of Neuroscience, 16*(23), 7733–7741.

Newsome, W. T., & Pare, E. B. (1988). A selective impairment of motion perception following lesions of the middle temporal visual area (MT). *The Journal of Neuroscience, 8*, 2201–2211.

Raymond, J. E. (1993). Complete interocular transfer of motion adaptation effects on motion coherence thresholds. *Vision Research, 33*(13), 1865–1870.

Rodman, H. R., & Albright, T. D. (1989). Single-unit analysis of pattern-motion sensitive properties in middle temporal visual area (MT). *Experimental Brain Research, 75*, 53–64.

Rose, D. (1980). The binocular: monocular sensitivity ratio for movement detection varies with temporal frequency. *Perception, 9*(5), 577–580.

Salzman, C. D., Murasugi, C. M., Britten, K. H., & Newsome, W. T. (1992). Microstimulation in visual area MT: effects on direction discrimination performance. *The Journal of Neuroscience, 12*, 2331–2355.

Schroder, J.-H., Fries, P., Roelfsema, P. R., Singer, W., & Engel, A. K. (1998). Correlates of strabismic amblyopia in cat extrastriate visual areas. *The European Journal of Neuroscience (Abstract), E10*, p237.

Schroder, J. H., Fries, P., Roelfsema, P. R., Singer, W., & Engel, A. K. (2002). Ocular dominance in extrastriate cortex of strabismic amblyopic cats. *Vision Research, 42*(1), 29–39.

Siegel, R. M., & Andersen, R. A. (1988). Perception of three-dimensional structure from motion in monkeys and man. *Nature (London), 331*, 259–261.

Simmers, A. J., Ledgeway, T., Hess, R. F., & McGraw, P. V. (2003). Deficits to global motion processing in human amblyopia. *Vision Research, 43*, 729–738.

Snowden, R. J., & Rossiter, M. C. (1999). Stereoscopic depth cues can segment motion information. *Perception, 28*(2), 193–201.

Williams, D. W., & Sekuler, R. (1984). Coherent global motion percepts from stochastic local motions. *Vision Research, 24*, 55–62.

Zeki, S. (1978). Functional specialization in the visual cortex of the rhesus monkey. *Nature, 274*, 423–428.